Warm Prestressing Effects in Notched Bars of a MnNiMo Steel Weld-metal

P. A. S. REED and J. F. KNOTT
Department of Materials Science, University of Cambridge, New Museum Site, Pembroke Street, Cambridge CB2 3QZ, UK

ABSTRACT

The effect of warm prestressing in notched specimens is found to be dependent on the fraction of general yield (GY) achieved in prestress i.e. on the size of the plastic zone. Little or no effect of prestress is observed if the fraction of GY at failure is not exceeded in prestress. Local stress distributions have been calculated for the specimens using the results of finite element analysis. Different types of prestress cycle have been investigated.

KEYWORDS

Warm Prestressing, inclusions, cleavage fracture, residual stress, fraction of general yield

INTRODUCTION

Warm prestressing (WPS) is a phenomenon which apparently toughens steels. Its operation is shown in Fig. 1. A sharply precracked specimen, if loaded in the upper shelf region to a stress intensity (K) higher than its lower shelf fracture toughness (K_{IC}) and then held at constant load and cooled, does not fracture as soon as the temperature drops below the ductile-brittle transition curve. It can be cooled to the lowest temperatures without fracture occurring and a further increase in load is required for failure to occur. This is known as the Load Cool Fracture cycle (LCF). Alternatively, if a specimen is similarly loaded in the upper shelf region (prestressed) but is then unloaded at the same temperature and cooled to the lower shelf, subsequent loading to failure shows an increase in the lower shelf fracture toughness, although the critical K-value is not as high as that applied in the prestress. This is known as the Load Unload Cool Fracture cycle (LUCF). These prestress effects are of interest, inter alia, in considering the integrity of pressure vessels under postulated loss-of-coolant-accidents. Thus, the extent of the WPS effect, and quantitative and qualitative models for it are of major interest. The regions of a pressure vessel of most concern with respect to brittle failure are the welds, and so an investigation into the effects of WPS in a representative weld-metal, A533BW, has been undertaken.

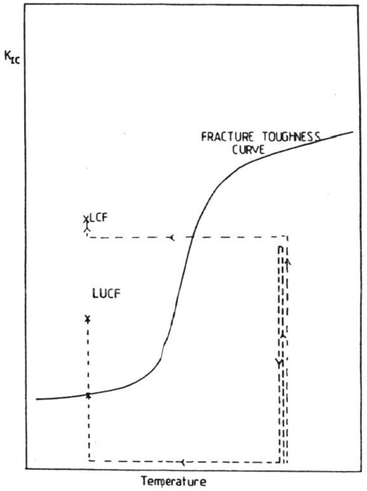

Fig. 1 Schematic WPS diagram

Notched test-pieces, rather than sharply precracked specimens, were used to explore the factors involved in WPS for the reasons outlined below: See also Harris *et al* (1986)

(1) The WPS loading does not produce any change in the notch profile which is significant with respect to subsequent low temperature fracture behaviour, and so any prestress effect witnessed in notched specimens will not be due to macroscopic precrack blunting. Previous studies on precracked specimens of A533BW (Reed and Knott, 1988) have, in fact, shown that such blunting is not a major effect.

(2) A blunt notch may be prestressed either in tension or compression to produce residual stress distributions of different signs.

(3) Since there is no fatigue crack, there are no stress distributions from the precracking operation to be taken into account in analysing any prestress effect.

A popular model for WPS in sharply cracked specimens is based on the superposition of stress fields, Chell (1980) and Curry (1979), and the notch geometry was chosen to be one for which elastic/plastic analyses are available (Griffiths and Owen, 1971; Wall and Foreman, 1985) so that the model could be tested for blunt notches.

Another possible mechanism for the WPS effect is the formation and blunting out of microcrack nuclei during prestress, thus effectively changing the "available" inclusion size distribution. See Fig. 2 (after Reed and Knott, 1988) where a smaller inclusion can be seen initiating a facet of cleavage near several larger inclusions which are seemingly blunted out. This was found to be a minor effect in the sharply precracked specimens investigated by Reed and Knott (1988)

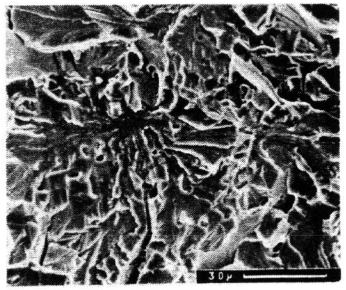

Fig. 2 Smaller inclusion initiating failure after prestress (Reed and Knott, 1988)

EXPERIMENTAL METHODS

It is important to establish the effect of WPS in a weld, despite the inherent difficulties caused by variation in microstructure and mechanical properties. Tests were performed on a submerged arc weldment (A533BW) of compostion 0.04wt% C, 1.26wt% Mn, 1.66wt% Ni, 0.35wt% Mo, 0.025wt% Cu, 0.002wt% S, 0.007wt% P, 0.65wt% Si, 0.08wt% Cr. The as-received heat treatment was as follows: 6hrs at 920^{o}C, Quench, followed by a combined temper and intermediate stress relief of 42 hrs at 600^{o}C, slow cooling to 300^{o}C followed by a final stress relief of 6 hrs at 650^{o}C and cooling in still air.

Two sets of specimens were machined in a comparable manner from two weldments of the same nominal composition and heat treatment. The orientation of test-pieces is shown (for the first set) in Fig. 3a.

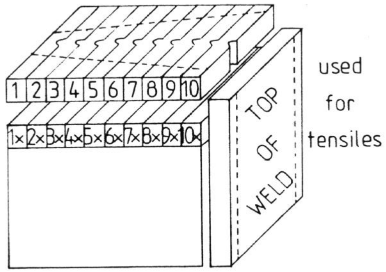

Fig. 3a Specimen orientation

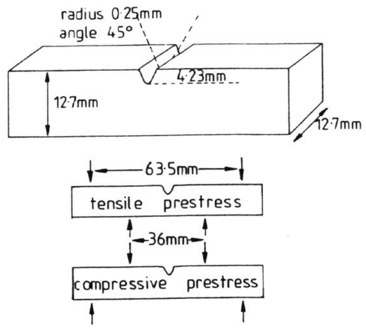

Fig. 3b Testpiece dimensions and loading configurations

All notched bar testing was performed in four point bend using a 100 kN Mand servohydraulic testing machine: see Fig. 3b for specimen dimensions and loading configurations. Prestressing and testing to failure was carried out at four temperatures: 20°C, -100°C, -150°C and -196°C; temperature control was maintained to within 2°C

An interesting finding from previous work (Harris *et al*, 1986) on WPS in notched bars is that prestressing at high temperature to *less than* the fracture load (P_F) at low temperature, can still give an *increase* in the subsequent P_F at the lower temperature. This is different from the conventional WPS diagram for sharply precracked specimens where the lower shelf K-value (nominally equivalent to P_F in the case of blunt notch specimens) has to be exceeded in the upper shelf if an increase in the subsequent fracture load is to be observed.

To investigate this further, a series of tests was run, in which three different prestress temperatures and three different prestress loads were employed, to investigate whether it was the fraction of GY in the prestress that determined the extent of toughness enhancement, or the prestress load (P_P) independent of prestress temperature. The prestress cycle used was LUCF (see Fig. 1) at three prestress temperatures 20°C, -100°C and -150°C. The prestressed specimens were subsequently loaded to failure at -196°C and load versus ramp displacement readings were monitored during prestress and final testing.

In a second series of tests the effect of changing the sign and type of the prestress cycle was investigated. To give a compressive prestress the second loading configuration shown in Fig. 3b was used. Similar prestress loads were used (23.7-24.8kN) at -100°C to give the same fraction of GY (1.00-1.12) and the effect on subsequent P_F at -196°C (in the tensile configuration) was noted. The LCF cycle was also investigated but this could be done only for the tensile configuration as it is impossible for a compressive prestress in the LCF cycle to be followed by tensile loading without an unloading step. Compressive prestress at -100°C was undertaken to equivalent loads, the specimen was then cooled to -196°C (i.e. the existing stress distribution was frozen in), unloaded, and changed to the tensile loading configuration under liquid nitrogen (to maintain the temperature at -196°C). It was then reloaded to failure. This is therefore a Load Cool Unload Fracture cycle (LCUF) in compression.

The fracture surfaces of broken specimens were examined, using a Camscan S4 scanning electron microscope.

RESULTS AND DISCUSSION

Baseline fracture data were obtained for non warm prestressed (NWPS) specimens tested at -196°C for comparison purposes. Specimens 1 and 2 were taken from weldment 1; D1, D4, D5 and D8 were taken from weldment 2 :

The variation of 0.2% proof stress with temperature was determined, (Fig. 4) using tensile specimens all taken from the top surface of the weld.

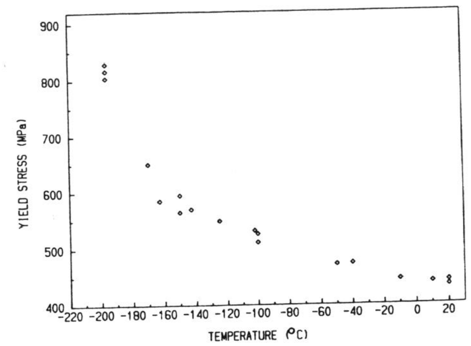

Fig. 4 Yield stress variation with temperature

A study of the variation of hardness across and down a block was made (Fig. 5). As can be seen from the diagram, the weld was undermatched to the parent plate hardness, but was harder on the top and bottom surfaces than in the centre. Therefore the (top surface) yield stress values obtained in Fig. 4 are slightly higher than would be expected for the average yield stress across the whole weld. Since yield stress is an important parameter, some account of this variation from specimen to specimen had to be made. Three Vickers hardness values (H_v) were taken close to the notch of each specimen and the assumption was made that the ratio of H_v values was equal to the ratio of yield stresses between specimens. Since yield stress and H_v values were known for the top surface of the weld, the variation in yield stress from specimen to specimen could be estimated.

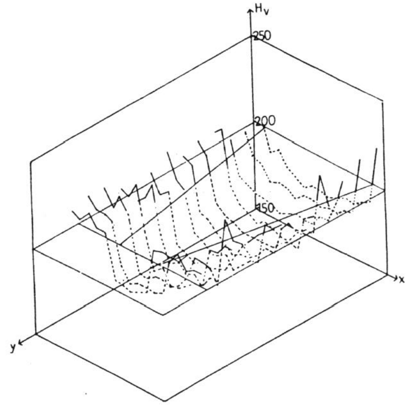

Fig. 5 H_v variation across weld

Table 1 - Baseline Pf values for NWPS specimens

Specimen no.	Definition	P_F (kN)	σ_{nom} (MPa)	σ_y (MPa)	R	σ_{max} (MPa)	fraction of GY	
1	NWPS	31.5	1426	817	2.38	1944	0.81	0.83
2	NWPS	30.2	1367	761	2.40	1826	0.84	average
D1	NWPS	27.5	1245	772	2.30	1776	0.75	
D4	NWPS	25.0	1132	744	2.24	1667	0.71	0.75
D5	NWPS	26.7	1209	705	2.36	1664	0.80	average
D8	NWPS	27.5	1245	776	2.29	1777	0.75	

Using the results of Griffiths and Owen (1971) it was possible to determine values of the maximum local tensile stress at failure, σ_{max}. In the absence of other information this was equated to σ_f*, the local cleavage fracture stress. The first set of specimens have a higher P_F and σ_F* at -196°C than the second set and break at a higher fraction of GY. In considering the magnitude of the WPS effect when both sets of specimens were used, the critical parameter was therefore the % change in fraction of GY (compared with baseline data set) on fracture at -196°C.

It is also possible to generate stress distributions at fracture for the NWPS specimens in Table 1 - see Fig. 6.

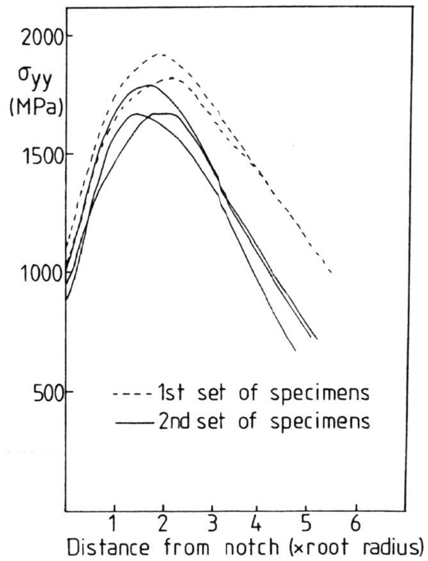

Fig. 6 NWPS stress distributions

From these stress distributions one would expect cleavage initiation to take place at the position of maximum tensile stress if fracture nucleation sites were abundant and uniformly distributed. Attempts were made to identify initiation sites using the SEM (often more than one initiation site could be seen) Some specimens showed initiation from inclusions (e.g. Fig. 7) but

sites were not always clearly visible, possibly because the weldment contained so many inclusions that the primary microcracking event was only slightly ahead of many secondary cracking events, or because initiation was not from an inclusion.

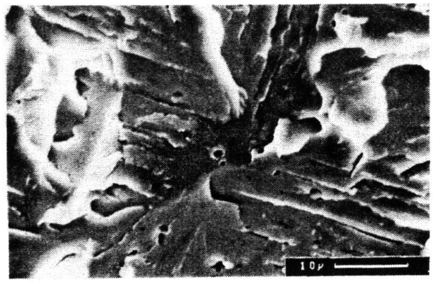

Fig. 7 Inclusion initiating failure

Table 2 compares both the theoretical positions of maximum tensile stress with the observed distances of initiation sites from the notch root (where these could be seen), and also the local tensile stresses at observed initiation sites with calculated values of σ_{max}.

Table 2 - Comparison of theoretical and observed initiation sites

Specimen no.	Position of max. tensile stress,	Extent of plastic zone	Distance from notch root of observed sites	σ_{max} (MPa)	σ_{yy} at observed sites (MPa), σ_f*
1	550 μm	1550 μm	380 μm	1944	1860
			370 μm		1855
2	500 μm	1600 μm	380 μm	1826	1750
			485 μm		1800
			515 μm		1810
D1	375 μm	1250 μm	559 μm	1776	1700
D4	375 μm	1140 μm	no clear sites	1667	-
D5	500 μm	1420 μm	423 μm	1664	1650
D8	375 μm	1250 μm	no clear sites	1777	-

The local stresses at the observed initiation sites are close to, but lower than the σ_{max} values, which implies that at the positions of peak tensile stress (σ_{max}), no suitable microcrack nuclei could be found, but that, not far from these positions, at slightly lower local stresses, suitable microcrack nuclei were present. The discrepancies between actual and assumed initiation sites, and between the local stress at observed sites and values of σ_{max} are due to the requirement for a "suitable" inclusion to be present at the peak tensile stress, i.e. on the spatial distribution and size distribution of inclusions. Both Tweed's (1983) and McRobie's (1985) work have shown the link between σ_f* and the size of available microcrack nuclei - which are sometimes but not always inclusions. A second point to note is that all observed initiation sites lie well within the plastic zone implying that plastic flow is required for cleavage to occur.

Results from the first series - Prestressing to different fractions of GY in the LUCF cycle.

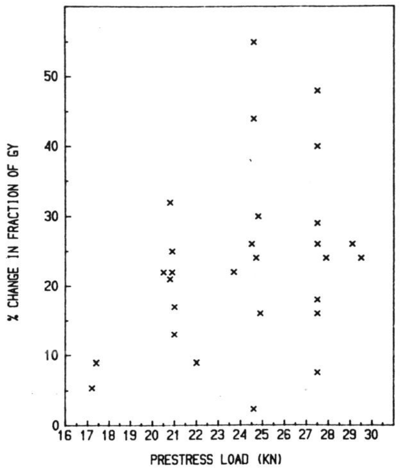

Fig. 8 P_P vs % change in fraction of GY on fracture (LUCF)

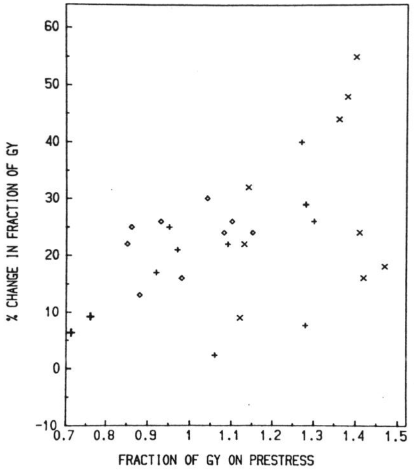

Fig. 9 Fraction of GY on prestress vs % change in fraction of GY (LUCF)

In Fig. 8 P_P has been plotted versus % change in fraction of GY and in Fig. 9 the fraction of GY on prestress has been plotted versus % change in fraction of GY. It can be seen that it is the fraction of GY on prestress that determines the extent of the WPS effect, rather than the P_P alone. There is still however a lot of scatter, which may arise from two effects: Firstly, there may be scatter due to the difference in the weldment's microstructure/inclusion distribution as sampled by different specimens. Secondly, prestressing to higher fractions of GY (i.e. above 1.0) gives rise to gross yielding of the specimen such that yielding from the top surfaces relieves the stress experienced at the notch.

From these results it can be seen that there is a definite WPS effect in notched specimens of A533BW - although the P_P is never greater than the NWPS P_F value. This is not observed for WPS of sharp-cracked specimens. From Fig. 9 it can be seen that if the fraction of GY at prestress is the same as, or less than, that at fracture for NWPS specimens, there is little or no WPS effect. Hence it is the fraction of GY at fracture in NWPS specimens that must be exceeded in prestress to produce a WPS effect in notched specimens. We conclude that the WPS effect relies on the principle that since the fraction of GY represents the size of plastic zone produced, the plastic zone size of the prestress step must exceed the plastic zone size of the NWPS fracture. This is similar in concept to the argument employed by Chell (1980) and Curry (1979) for precracked specimens.

Second series - Investigation of LCF and LUCF cycles with different signs of prestress.

Table 3

Specimen no.	Prestress cycle	fraction of GY on prestress	P_F (kN)	fraction of GY on fracture	%change in fraction of GY	
5	LCF(tens)	1.04	34.7	0.98	+18%	
6	LCF(tens)	1.20	35.2	0.98	+18%	} +24%
B2	LCF(tens)	1.10	35.9	1.03	+37%	
9	LCUF(comp)	1.05	15.4	0.42	-49%	
4x	LCUF(comp)	1.10	13.4	0.39	-53%	} -50%
B4	LCUF(comp)	1.15	13.2	0.38	-49%	
3	LUCF(tens)	1.30	35.6	1.04	+25%	
4	LUCF(tens)	1.00	37.1	1.01	+22%	} +17%
A8	LUCF(tens)	1.05	28.5	0.77	+3 %	
7	LUCF(comp)	1.12	23.1	0.62	-25%	
8	LUCF(comp)	1.10	24.9	0.69	-17%	} -31%
B3	LUCF(comp)	1.12	12.6	0.36	-52%	

The compressive cycles (giving rise to tensile residual stresses) seem to be more effective in reducing P_F than are the tensile cycles in increasing P_F, Harris *et al* (1986) found this to be the case in their investigation of the LUCF cycle and explained it in terms of stress distribution superposition: as load increases, the peak tensile stress moves progressively away from the notch root (Fig. 10), local tensile residual stresses (from the compressive prestress) superimpose on stress applied at -196°C and promote failure close to the notch at low applied load. The compressive residual stress will also superimpose near to the notch root (and compensate) but as the peak applied tensile stress moves progressively away from the notch root the compressive residual stress decreases, and therefore contributes less to the enhancement of toughness.

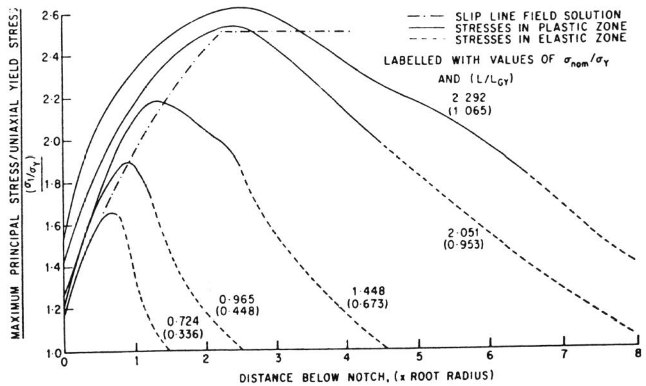

Fig. 10 Variation of σ_{yy} below the notch root at various loads (Griffiths and Owen, 1971)

The compressive LCUF cycle is more deleterious than the LUCF cycle and this can also be explained in terms of the superposition of stress distributions from the loading, unloading and reloading steps. If the same prestress loading operation takes place, to a given fraction of GY, then unloading at the same temperature and at a lower temperature will give two different residual stress distributions. When a specimen unloads from a certain fraction of GY it has an effective yield stress equal to the compressive yield stress put in by the loading plus the yield stress in tension at the unloading, so for the LUCF cycle, the effective yield stress for the unloading step is $2\sigma_p$, and for the LCUF cycle is $(\sigma_p + \sigma_f)$, where σ_p is the yield stress at prestress and σ_f is the yield stress at failure. Since $\sigma_f > \sigma_p$ and the normalised stress distribution is given in terms of σ_{yy}/σ_y it can be seen that for the LUCF cycle the unloading stress distribution (from the same fraction of GY) will be lower than that for the LCUF cycle, and hence will give rise to smaller residual compressive stresses. From this reasoning a tensile LCUF cycle will give a greater increase in subsequent P_F than a tensile LUCF cycle prestressed to the same level.

CONCLUSIONS

(1) A WPS effect is observed in blunt notch specimens and thus clearly shows that for A533BW the prestress effect cannot be solely due to blunting of the crack-tip.

(2) The P_P never exceeded the NWPS P_F and yet an effect was observed, contrary to conventional depictions of the WPS effect. It was noted however that the fraction of GY on prestress exceeded the fraction of GY on failure for NWPS specimens for a prestress effect to be observed. Since the fraction of GY gives a measure of the plastic zone size, then the plastic zone on prestress must exceed the plastic zone on failure to give a prestress effect, which agrees with the theories of Chell (1980) and Curry (1979)

It was found that the greater the fraction of GY on prestress, the greater the prestress effect, although a fair amount of scatter was seen with greater prestress.

(3) Using the Griffiths and Owen (1971) stress distributions for specimens of the geometry used, it was possible to calculate values of σ_f^* which were not necessarily found at the positions of peak tensile stress for NWPS specimens. This indicated the effect that the spatial distribution and size distribution of the inclusions can have on the fracture properties of such weld metals.

(4) The decrease observed in subsequent P_F values after a compressive LUCF cycle was greater than the increase observed after a tensile LUCF cycle. This could be explained in terms of the superposition of the final loading stress distribution on residual stresses generated by the prestress. The greater effectiveness of the LCUF compressive cycle compared with the LUCF compressive cycle can also be explained in terms of the superposition of stress distributions.

ACKNOWLEDGEMENTS

Thanks are due to Professor D. Hull for the provision of laboratory facilities.

REFERENCES

Chell, G.C. (1980). *Proc. 4th Int. Conf. Pres. Ves. Tech.*, Vol.1, Inst. Mech. Eng., London

Curry, D.A., (1979). *CERL Report No.RD/L/N 103/79*, Leatherhead, U.K.

Griffiths, J.R. and D.R.G. Owen (1971). *J. Mech. Phys. Sol.*, Vol.19,

Harris, C.P., P. Bowen and J.F. Knott (1986). *Proc. 6th Eur. Conf. on Fract., Amsterdam*

McRobie, D.E. (1985). *Cleavage Fracture in C-Mn Weld Metals*, Ph.D., University of Cambridge

Reed, P.A.S. and J.F. Knott (1988) *Proc. 7th Eur. Conf. on Fract., Budapest*

Tweed, J.H. and J.F. Knott (1983). *Met. Sci.*, Vol. 17

Wall, M. and A.J. Foreman (1985). *Harwell Report, R11618*, UKAEA